
Do Large Scale Molecular Language Representations Capture Important Structural Information?

Jerret Ross, Brian Belgodere, Vijil Chenthamarakshan
Inkit Padhi, Youssef Mroueh, Payel Das*
IBM Research AI

Abstract

Predicting chemical properties from the structure of a molecule is of great importance in many applications including drug discovery and material design. Machine learning based molecular property prediction holds the promise of enabling accurate predictions at much less complexity, when compared to, for example Density Functional Theory (DFT) calculations. Features extracted from molecular graphs, using graph neural nets in a supervised manner, have emerged as strong baselines for such tasks. However, the vast chemical space together with the limited availability of labels makes supervised learning challenging, calling for learning a general-purpose molecular representation. Recently, pre-trained transformer-based language models (PTLMs) on large unlabeled corpus have produced state-of-the-art results in many downstream natural language processing tasks. Inspired by this development, here we present molecular embeddings obtained by training an efficient transformer encoder model, referred to as MOLFORMER. This model was employed with a linear attention mechanism and highly parallelized training on 1D SMILES sequences of 1.1 billion unlabeled molecules from the PubChem and ZINC datasets. Experiments show that the learned molecular representation performs competitively, when compared to existing graph-based and fingerprint-based supervised learning baselines, on the challenging tasks of predicting properties of QM8 and QM9 molecules. Further task-specific fine-tuning of the MOLFORMER representation improves performance on several of those property prediction benchmarks. These results provide encouraging evidence that large-scale molecular language models can capture sufficient structural information to be able to accurately predict quantum chemical properties and beyond.

1 Introduction

Supervised learning on molecules has tremendous potential in chemistry, drug discovery, and materials science. Quantum mechanical (QM) calculations with approximations allow computation of molecular properties; different approximations of theory, e.g. Density Functional Theory (DFT) with varying level of functionals, is used to achieve a reasonable trade-off between accuracy and speed. Machine learning has emerged as an appealing alternative as a computationally efficient approach. Machine learning (ML) models for molecules can be trained directly on a set of pre-defined chemical descriptors. Some of the popular ML models in this class have used hand-derived derivatives of geometric features such as Coulomb Matrix (CM) [Rupp et al. \(2012a\)](#), or a combination of nuclear charges and atomic distance matrix [Schütt et al. \(2017\)](#). In contrast, more recent ML models have focused on automatically learning the features from the natural graphs that encode the connectivity information, or the line annotations of molecular structures, such as the popular SMILES (simplified molecular input line entry system) representation [Weininger \(1988\)](#). SMILES defines a character

*Correspondence to rossja@us.ibm.com

string representation of a molecule by performing a depth-first pre-order traversal of a spanning tree of the molecular graph, generating symbols for each atom, bond, tree-traversal decision, and broken cycles. The resulting character string therefore corresponds to a flattening of a spanning tree of the molecular graph. Learning on SMILES has been widely adopted for molecular property prediction [Goh et al. \(2017\)](#); [Öztürk et al. \(2018\)](#); [Paul et al. \(2018\)](#); [Shin et al. \(2019\)](#), as SMILES is generally more compact compared to most other methods of representing structure, including graphs. Additionally, meaningful substructures such as branches, cyclic structures, and chirality information are explicitly represented in SMILES strings, which is not the case for the graph representation. However, the SMILES grammar is complex and restrictive; most sequences over the appropriate character set do not belong to well-defined molecules. Further, SMILES are thought not to be topology-aware while graphs are. Due to these limitations, deep models may focus their learning on the SMILES grammar and not the implicit topological structure. Accordingly, while SMILES representation learned using deep neural nets has been employed in predicting the biochemical properties [Öztürk et al. \(2018\)](#); [Paul et al. \(2018\)](#); [Shin et al. \(2019\)](#); [Jo et al. \(2020\)](#), its ability toward predicting QM properties, that are strongly tied with a low energy 3D structure (also referred as conformer), has been less explored.

In contrast, Graph Neural Networks (GNNs) [Gori et al. \(2005\)](#); [Duvenaud et al. \(2015a\)](#) and their variants including [Duvenaud et al. \(2015b\)](#); [Defferrard et al. \(2017\)](#); [Kipf and Welling \(2017\)](#); [Li et al. \(2015\)](#); [Veličković et al. \(2018\)](#); [Hamilton et al. \(2018\)](#); [Gilmer et al. \(2017\)](#); [Schlichtkrull et al. \(2017\)](#); [Liao et al. \(2019\)](#); [Chen et al. \(2019\)](#) have been extensively used and shown impressive performance for learning molecular representations on QM property prediction. GNN frameworks can be generically viewed as “message passing”, which includes local neighborhood information aggregation and information update across different levels of granularity, e.g. nodes, edges, or the full graph, according to the graph’s connectivity structure.

Recent success of language representation models in downstream NLP tasks, as obtained by combining the power of pre-training on large unlabeled corpus and contextual language models (LMs) using advanced neural nets like Transformers [Vaswani et al. \(2017\)](#), has inspired extending this paradigm to other domains, where domain-specific “language” embeddings obtained using pre-trained LMs were exploited as the exclusive input for several subsequent tasks. While pre-trained LMs for molecules started to emerge for biochemical property predictions, to date there is no report on how those molecular LMs trained at large scale perform on QM target predictions, which requires capturing the subtle relationship between 3D conformers and electronic properties. Here we present transformer models of molecular SMILES, obtained using efficient linear attention mechanism and trained on a large corpus of 1.1 billion molecules, referred as MOLFORMER (Molecular Language transformer). Our experiments on QM9 and other benchmark datasets show, for the first time, that pre-trained transformer encoders of molecular SMILES perform competitively with geometry and graph-based NNs, suggesting pretrained and contextualized molecular LMs are able to capture, at least to some extent, the implicit relation between a low energy 3D conformation and resulting properties, without having access to the 3D coordinates or the graph topology of molecules.

Our main contributions are

- We train a large scale and efficient Molecular Language model transFormer (MOLFORMER) on over a billion molecules, with relatively limited hardware resources (up to 16 V100 GPUs). We owe our scalability and speedups to efficient linear time attention, adaptive bucketing of batches, and open source parallelization provided in PyTorch Lightning [Falcon \(2019\)](#) and NCCL. Without the combination of bucketing and linear attention we would be limited to a batch size of less than 50 per GPU, requiring us to use over 1000 GPUs to achieve the same wall clock time.
- We explore the difference between absolute and relative position embeddings, in representing molecular SMILES. We also provide a new efficient and accurate linear attention approximation of the recently proposed relative position Roformer.
- We perform extensive experimentation and ablation studies on using MOLFORMER for predicting Quantum Mechanical properties on the popular QM8 and QM9 benchmark datasets.
- Our results provide encouraging evidence that MOLFORMER representations can capture sufficient structural information to be able to accurately predict quantum chemical properties and beyond. The performance of MOLFORMER is on par with more specialized models that

leverage more expensive and precise 3D information as input, while MOLFORMER learns from readily available SMILES annotations.

2 Related Work

Large Scale Training of Language Model The recent advancement of transformer-based masked language models (MLMs) Liu et al. (2019b); Devlin et al. (2019) and prefix language models (PLMs) Raffel et al. (2020a) have shown remarkable performance on various natural language understanding tasks. Unsupervised pre-trained representation learning of sequences through MLMs, randomly masks input tokens during training and then predicts these masked tokens. Whereas, PLMs require adding task-specific text tags to the input sequences. These language models show substantial scalability through increasing transformer models size and training using large-scale data corpora. Moreover, recent efforts to address the challenges of memory usage and costs incurred in modeling long-range dependencies as sequence length increases. Different efficient transformers introduced through Choromanski et al. (2020); Beltagy et al. (2020); Kitaev et al. (2020); Wang et al. (2020) address the quadratic memory challenges within the self-attention mechanism.

Molecular Representation Learning To represent molecules in vector space, traditional chemical fingerprints such as ECFP Rogers and Hahn (2010), have been used to encode neighboring atoms of a molecule into a fixed-length vector. Convolutional layers have also been used to learn the neural fingerprints of molecules Duvenaud et al. (2015a); Coley et al. (2017). Following these methods, RNN-based models have been used for molecular representation learning using SMILES and other linear molecular annotations as inputs Bjerrum (2017). More recent directions involve graph convolutional networks which encode molecular graphs into neural fingerprints. To better capture the interactions among atoms, Gilmer et al. (2017) proposed the message passing framework Kipf and Welling (2017); Schütt et al. (2017). Many variations of the original message passing concept aimed at learning nonlocal effects; for instance, Xiong et al. (2019) introduced an attention mechanism. Most of these message passing neural nets (MPNNs) operate on 2D topological graphs; however, a few works also incorporated the 3D positional information when performing the aggregation and update processes Schütt et al. (2017); Unke and Meuwly (2019); Klicpera et al. (2020); Liu et al. (2021). One challenge faced by MPNNs is achieving higher expressivity that can distinguish between two given graphs to that of the hierarchy of the Weisfeiler-Lehman (WL) graph isomorphism, while maintaining scalability. It has been shown that message passing models have limited expressiveness and are not better than the first WL test (1-WL) Morris et al. (2019). Morris et al. have developed powerful deep models generalizing message passing to higher orders that are as expressive as higher order Weisfeiler-Lehman (WL) isomorphism tests Morris et al. (2019), at the cost of high computational expense. Permutation equivariant operators on the tensors that represent k-order interactions between graph nodes has been suggested as an alternative to message passing, which has been shown to have more expressive power Maron et al. (2020).

Pretrained Language and graph Models for molecules Recent success of language representation models in downstream NLP tasks, as obtained by combining the power of pre-training on large unlabeled corpus and contextual language models (LMs) using advanced neural nets like Transformers, has inspired extending this paradigm to other domains, where a domain-specific "language" embeddings obtained using PTMs were exploited as the exclusive input for several subsequent tasks. One such example is understanding the language of life through advanced LMs trained on protein sequences, in which features extracted by LMs directly from single protein sequences reach state-of-the-art performance in downstream prediction tasks, even when those were used without evolutionary information Vig et al. (2020); Rives et al. (2020); Elnaggar et al. (2021). Similar large-scale unsupervised pre-training on SMILES sequences has been explored for molecular property prediction Chithrananda et al. (2020); Xue et al. (2020); Wang et al. (2019); however, those models did not attempt to predict quantum chemical properties. Unsupervised representation learning has been tested on molecular graphs as well Liu et al. (2019a); Rong et al. (2020). To our knowledge, the present study is the first one that explores the representational power of pre-trained molecular language models on predicting downstream quantum mechanical targets for which learning the molecular structural information is known to be crucial.

3 Large Scale and Efficient Pretrained Molecular Language Models

The dataset that we use for this paper is a combination of the PubChem [Kim et al. \(2018\)](#) and ZINC [Irwin and Shoichet \(2005\)](#) databases. PubChem consists of 111 million molecules, while the much larger ZINC dataset contains 1 billion molecules. To construct a vocabulary we utilize the tokenizer from [Schwaller et al. \(2019\)](#). Running this tokenizer on molecules converted to the canonical form utilizing RDKit [RDKit \(online\)](#), we end up with a vocabulary size of 2357 characters plus 5 special characters, totalling up to 2362 characters for the combined PubChem+ZINC. The sequence length range generated after tokenizing all molecules in the combined dataset range from 1 to just over 2000 characters. We decide to limit our sequence length range from 1 characters to 202 characters, special characters inclusive, to reduce computation time. We assumed that this would have minimal impact on training due to over 99.4 percent of all molecules from our dataset containing less than 202 characters.

3.1 Efficient Transformer Encoder with Linear Attention

One of the computational bottlenecks in transformers [Vaswani et al. \(2017\)](#) is that attention has a quadratic computational cost with respect to sequence length. Linear complexity attention models [Katharopoulos et al. \(2020\)](#); [Choromanski et al. \(2020\)](#) tackled this issue, via kernel approximations using variants of random features approximations.

Aiming at performing large scale Masked Language Model training efficiently utilizing relatively limited hardware resource, we decided to experiment with an encoder transformer with Linear attention [Katharopoulos et al. \(2020\)](#). Our model consists of 12 layers, 12 attention heads per layer and has a hidden state size of 768. A Generalized Feature map [Katharopoulos et al. \(2020\)](#) for the linear attention was chosen after preliminary experiments showed an acceptable balance between computation speedup and minimal performance reduction when compared to the FAVOR [Choromanski et al. \(2020\)](#) feature map. Generalized features are a simplification of the feature map in FAVOR [Choromanski et al. \(2020\)](#). The Generalized map removes the softmax approximation but it can increase the rank of the resulting attention matrix. The size of the feature map is 32.

3.2 Position Embeddings and Fast Linear RoFormer

The seminal work of [Vaswani et al. \(2017\)](#) considered absolute position embeddings to encode the position of a token in the sequence. [Shaw et al. \(2018\)](#); [Raffel et al. \(2020b\)](#); [Ke et al. \(2021\)](#) showed that using relative position embeddings between tokens results in better performance. Rotary position embeddings were introduced recently in RoFormer of [Su et al. \(2021\)](#) as a means to enhance relative encoding via position dependent rotations R_m of the query and the keys at a position m . These rotations can be efficiently implemented as pointed-wise multiplications and don't result in cumbersome computations.

In order to leverage Rotary embeddings with linear transformers [Su et al. \(2021\)](#) proposed the use of the following approximation :

$$\text{Attention}_m(Q, K, V) = \frac{\sum_{n=1}^N \langle R_m \varphi(q_m), R_n \varphi(k_n) \rangle v_n}{\sum_{n=1}^N \langle \varphi(q_m), \varphi(k_n) \rangle},$$

where Q, K, V are the query, key and value respectively, and φ a random feature map.

After a preliminary experimentation with this fast Roformer, we found it to be behind its absolute position counterpart. We propose the following linear attention for Roformer that we found to train gracefully:

$$\text{Attention}_m(Q, K, V) = \frac{\sum_{n=1}^N \langle \varphi(R_m q_m), \varphi(R_n k_n) \rangle v_n}{\sum_{n=1}^N \langle \varphi(R_m q_m), \varphi(R_n k_n) \rangle}.$$

When compared with [Su et al. \(2021\)](#) we rotate the original keys and queries instead of the transformed ones with the feature map φ . We saw increased stability and faster convergence in training loss behavior on both PubChem and PubChem+ZINC when using rotary embeddings over absolute embeddings as observed in Figure 1.

3.3 Large Scale Training and Parallelization

Masked LM Training For pretraining we use the masked language model method defined in [Devlin et al. \(2018\)](#), 80% of the time a character will be replaced with the mask token, 10% of the time the character will be replaced with a random character and 10% of the time the character will be unchanged. For optimization we decided to use the Fused Lamb optimizer from [You et al. \(2019\)](#) as implemented via APEX [APEX \(online\)](#). This decision was made due to lambs ease of use for training. For example learning rate warm ups were found to be unnecessary and training was found to be robust when large batch sizes were used. All other optimizers were unable to maintain their stability without large amounts of modification any time a training configuration needed to be changed. Training took place for 4 epochs through the entire PubChem+ZINC dataset with a fixed learning rate of $1.6e^{-4}$ and a batch size of 1600 molecules per GPU on a total of 16 GPUs over 2 servers connected via Infiniband fabric, it should be noted that as the number of GPUs utilized increased we found an increase in learning rate was necessary up to a factor of 8.

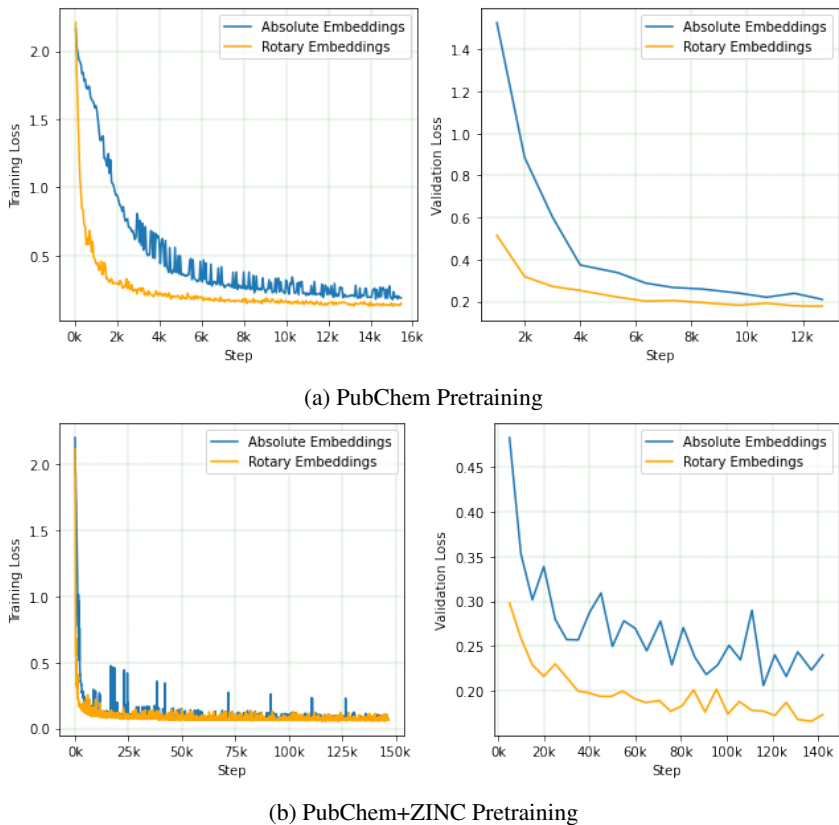


Figure 1: Training and validation losses of our Linear attention MOLFORMER with *rotary* (relative) and absolute position embeddings on a) PubChem and b) PubChem+ZINC (>1 billion data points). We see that both rotary and absolute MOLFORMER have graceful training curves. Our Rotary Linear attention MOLFORMER leads to lower training and validation losses than MOLFORMER with absolute position embeddings.

Faster Training with Adaptive Bucketing By Sequence Length We observed that the distribution of molecule lengths in our dataset centered around molecules that were less than 45 characters long after tokenization. This fact coupled with large batch sizes increased the likelihood that padding tokens would overwhelm each batch and result in large amounts of computational waste. To get around this problem we decided to break each minibatch into multiple buckets. Buckets were defined by sequence interval length, The first bucket would contain SMILES strings of length 1 to 42, the next bucket would be of size 43 to 66, the third bucket would be of size 67 to 122 and finally the last bucket would be of size 123 to 202. Due to the length distribution of our dataset buckets 1 and 2 would always be present in all training steps while bucket 3 would be present for the majority of

minibatches. Molecules that fell into bucket 4 appeared in most minibatches but would usually only represent a very small number of molecules found within the minibatch. Since this was true we decided to not utilize bucket 4 in the training procedure until it reached a threshold of 50 molecules. This method prevented us from training on a bucket that consistently contained a very small amount of molecules which we believe aided training. Bucketing combined with gradient accumulation across buckets gave us stable training while reducing computational time need over the traditional idea of keeping GPU memory full at all times to maximize compute regardless of the unneeded computation that arises due to the padding required given such a method. To be more concrete, without bucketing on 1 V100 GPU and on PubChem only a single epoch would take approx. 1200 hours while with bucketing the same epoch only took around 60 hours. This means that our adaptive bucketing leads in this case to $3.3\times$ speedup in training. A similar concept, namely micro-batching [Team \(2020\)](#) exists but we became aware of after implementing our adaptive bucketing technique. We have not yet baselined the differences between our domain specific bucketing implementation towards molecular data and the generic micro-batching of [Team \(2020\)](#).

Using Linear attention and bucketing allowed us to reduce the number of GPU needed for quadratic attention and no bucketing from roughly 1000 to 16.

Parallelization and Computing Environment All experiments were performed on a GPU cluster where each node contains either 8 NVIDIA Tesla V100 (32GB) or 8 Ampere A100 (40GB) GPUs connected via NVLink. The V100 nodes are equipped with dual 28-core (Intel Xeon Gold 6258R) CPUs, the A100 nodes are equipped with dual 64-core (AMD EPYC 7742) CPUs, and all nodes are connected by 2 non-blocking EDR InfiniBand (100Gbps) network adapters as well as 2 100Gbps Ethernet adapters. All nodes are installed with RHEL 8.3, CUDA 10.2, and cuDNN 7.5.

Due to the size of the datasets utilized in pretraining, our training environment relies on the Distributed Data Parallel functions provided by Pytorch [Paszke et al. \(2019\)](#) and Pytorch Lightning utilizing the NCCL backend. By utilizing RDMA to enable GPU-direct technology we were able to efficiently scale to multi-node multi-GPU training. Additionally, we utilized HuggingFace Datasets [Wolf et al. \(2020\)](#) to localize the data onto the machines where pretraining took place to improve performance during pretraining. Our pretraining task consists of training on the full dataset to 4 epochs. Training a single epoch of just PubChem on a single NVIDIA V100 GPU would take approximately 60 hours. Utilizing Distributed Data Parallel, pretraining on the full PubChem dataset alone took approx. 22 hours on 16 NVIDIA V100 GPUs this averages to about 5.5 hours per epoch. The speed up achieved by parallelizing training to 16 GPUs gave us a factor of 10.9. Pretraining for 4 epochs on the combined PubChem+ZINC datasets took approx. 208 hours on a 16 NVIDIA V100 GPUs which averages to about 52 hours of compute for a single epoch. All finetuning tasks were able to be performed on single GPUs (either V100 or A100) and completed in approx. 12 hours.

4 Experimental Results

4.1 MOLFORMER embeddings

We encode a molecule by extracting the CLS embedding from the encoder model. The CLS embedding comes from the first embedding of the last hidden state of the encoder model. For downstream tasks we use the raw CLS embedding and omit any pooling methods. Two strategies are used for downstream tasks – the first strategy (Frozen) is to train a fully connected model for each task while keeping the encoder embeddings fixed. The second strategy is to fine tune the weights of the encoder model jointly with the fully connected model for each downstream task. The ideal configuration and hyperparameters for the first strategy is identified through a grid search as described in the supplemental material. For the second strategy, we use a 2 layer fully connected network with hidden dimension of 768 (matching the encoder embedding) with Dropout (set to 0.1) and ReLU layers in-between, on top of a final single output dimension for regression tasks.

4.2 Performance of MOLFORMER embeddings on Downstream Tasks

We evaluate the performance of MOLFORMER embeddings on several downstream tasks given below.

QM9 Tasks Here we evaluate the MOLFORMER performance on 12 regression tasks from the QM9 Quantum Mechanics benchmark dataset, consisting of approximately 134k organic molecules

with up to nine heavy atoms from carbon, oxygen, nitrogen and fluorine. As recommended by Wu et al. (2018), we use a random split consisting of 80%, 10% and 10% of the molecules for train, validation and test.

We compare the performance of our model with existing baseline models that fall in the following two classes: (1) Geometry-based models that encode Coulomb Matrix (CM) Rupp et al. (2012b) and its variants, as in deep tensor neural net (DTNN) Schütt et al. (2017), which are trained on pairwise atom distances in the 3D Euclidean space. (2) Graph neural nets - that considers topological information. Here we consider the MPNN Gilmer et al. (2017), Attentive-FP Xiong et al. (2019) and baseline GNN models that are more powerful than 1-WL, including 123-gnn Morris et al. (2019) and PPGN Maron et al. (2020). Results reported in Table 1 show that, though there is a consensus in the community that SMILES does not explicitly encode geometric or topological information, MOLFORMER with task-specific fine-tuning trained on SMILES strings of large molecular corpus achieves comparable or better performance to that of the majority of the competitors. Specifically, MOLFORMER outperforms geometry-based models (CM, DTNN) and GNNs with limited expressivity (MPNN, A-FP) in most of the tasks. GNNs that are more expressive, like 123-GNN and PPGN, perform better than MOLFORMER; however, those powerful networks are known to be difficult to scale - e.g. PPGN has a cubic time complexity (see Vignac et al. (2020)). As a comparison, the linear attention employed in MOLFORMER ensures a linear time complexity.

Measure	Geometry-Based		Graph-Based				SMILES-Based
	CM	DTNN	MPNN	A-FP	123-gnn*	PPGN*	MOLFORMER
α	0.85	0.95	0.89	0.492	0.27	0.382	0.4324
C_v	0.39	0.27	0.42	0.252	0.0944	0.184	0.1584
G	2.27	2.43	2.02	0.252	0.0469	0.238	0.8680
gap	0.0086	0.0112	0.0066	0.00528	0.0048	0.00406	0.0039
H	2.27	2.43	2.02	0.893	0.0419	0.229	1.1293
ϵ_{homo}	0.00506	0.0038	0.00541	0.00358	0.00337	0.00276	0.0030
ϵ_{lumo}	0.00645	0.0051	0.00623	0.00415	0.00351	0.00287	0.0025
μ	0.519	0.244	0.358	0.451	0.476	0.231	0.4035
$\langle R^2 \rangle$	46.00	17.00	28.5	26.839	22.90	16.07	20.5663
U_0	2.27	2.43	2.05	0.898	0.0427	0.234	0.4244
U	2.27	2.43	2.00	0.893	0.111	0.234	1.445
ZPVE	0.00207	0.0017	0.00216	0.00207	0.00019	0.00064	0.0004
Avg	4.7384	2.3504	3.1898	2.5820	1.9995	1.4843	2.1197

Table 1: MOLFORMER performance on QM9 test set. Our best MOLFORMER variant is pretrained on PubChem+ZINC dataset and finetuned for each measure. Baseline performance values are taken from Wu et al. (2018); Xiong et al. (2019); Maron et al. (2020). **Blue** indicates best performing model, while the value **in orange** indicates second-best, for each task. MOLFORMER trained with rotary embeddings on PubChem+ZINC stands out as a competitive model when considering both *regression performance and scalability*, in comparison to distance based NNs and GNNs with either limited or higher (indicated with “*”) expressivity.

Effect of dataset size and diversity on MOLFORMER performance We also investigate the effect of training sample size and diversity on MOLFORMER performance. Figure 2 shows the MAE change with varying training data sizes for the U_0 -Atom measure on the QM9 dataset, as obtained from the Moleculenet benchmarking suite. For reference, the standard deviation for U_0 -Atom measure of the test split is 239.75. Tables 2 and 3 report MAEs on QM9 regression tasks for a set of MOLFORMER variants, in terms of the positional embedding – regular or rotary used, and whether task-specific fine-tuning was performed or not. We also present MOLFORMER variants that are trained on (1) only QM9 training set (111k) – referred as MOLFORMER-qm9, (2) only PubChem (111M) – referred as MOLFORMER-pubchem, and compare their performance with MOLFORMER variants trained on PubChem+ZINC data – referred as MOLFORMER-XL. Results show that the performance based on average MAE varies in the following order: MOLFORMER-pubchem < MOLFORMER-qm9 < MOLFORMER-XL, confirming that unsupervised pre-training on a larger and diverse corpus enhances the representational power of the model, as showcased by its stronger performance on the

Pretraining Data → Measure ↓	QM9 Only			PubChem+ZINC		
	Frozen × Rotary	Finetuned × Rotary	Finetuned ✓ Rotary	Frozen × Rotary	Finetuned × Rotary	Finetuned ✓ Rotary
α	1.6258	0.5078	0.6001	0.5312	0.4324	0.3675
C_v	1.0176	0.1589	0.1906	0.2303	0.1584	0.1484
G	3.2528	0.9985	0.7479	0.3066	0.8680	1.0273
gap	0.0187	0.0057	0.0061	0.0085	0.0039	0.0038
H	1.9221	1.1579	1.0250	0.3675	1.1293	0.7283
ϵ_{homo}	0.0115	0.0042	0.0046	0.0062	0.0030	0.0029
ϵ_{lumo}	0.0157	0.0041	0.0056	0.0058	0.0025	0.0027
μ	0.8394	0.4380	0.4630	0.6463	0.4035	0.3787
$\langle R^2 \rangle$	86.9461	24.0785	25.9482	27.5962	20.5663	23.3702
U_0	3.0626	1.1462	1.3168	0.4500	0.4244	1.1215
U	1.8555	1.0454	1.6158	0.4480	1.4450	1.1110
ZPVE	0.0020	0.0011	0.0012	0.0004	0.0004	0.0004
Avg MAE	8.3808	2.4621	2.6604	2.5497	2.1197	2.3552
# Wins for fixed data	0	10	2	3	3	6

Table 2: Comparison of different MOLFORMER variants on QM9 test set. Models on the left half of the table are pre-trained using QM9 only, whereas the models on right half are pre-trained on PubChem+ZINC dataset. The variants with (✓) and without (×) rotary embeddings are compared. Our best candidate variant (for Table 1) is picked based on the average MAE score.

Measure ↓	Frozen × Rotary	Finetuned × Rotary	Finetuned ✓ Rotary
α	1.5470	0.5280	0.8452
C_v	0.9984	0.1506	0.2701
G	2.0089	0.8626	1.5920
gap	0.0182	0.0050	0.0109
H	2.3627	1.3342	0.7088
ϵ_{homo}	0.0147	0.0038	0.0082
ϵ_{lumo}	0.0148	0.0036	0.0080
μ	0.8509	0.4284	0.6166
$\langle R^2 \rangle$	87.2816	30.2904	34.0425
U_0	2.0613	0.8969	1.5503
U	1.9638	1.1122	1.1351
ZPVE	0.0020	0.0008	0.0012
Avg	8.260	2.968	3.399
# Wins for fixed data	0	12	0

Table 3: Comparison of MOLFORMER variants on QM9 test set of models pre-trained on PubChem data only.

QM9 benchmark. It is worth noting that MOLFORMER-XL without any rotary embedding (reported in Table 1) performs well based on the average MAE across all tasks, which is influenced mostly by $\langle R^2 \rangle$ measure. However, in majority of tasks MOLFORMER-XL with rotary embedding gives significant improvement in comparison to MOLFORMER-XL with regular embedding.

Downstream Tasks - QM8, Esol, & FreeSolv Table 4 documents the results of MOLFORMER-XL with regular positional embedding, along with two other GNN baselines, MPNN and A-FP, on three regression benchmark datasets - QM8, ESOL, and FreeSolv. QM8 [Ruddigkeit et al. \(2012\)](#); [Ramakrishnan et al. \(2015\)](#) consists of four excited state properties, each calculated by three different quantum mechanical methods, on 22k samples comprised of up to eight heavy atoms. ESOL [Delaney \(2004\)](#) is comprised of logarithmic aqueous solubility (mols/L) for 1128 organic small molecules. FreeSolv [Mobley and Guthrie \(2014\)](#) contains the calculated and experimental hydration free energies (kcal/mol) for 642 small neutral molecules in water. For all these tasks, we use a random

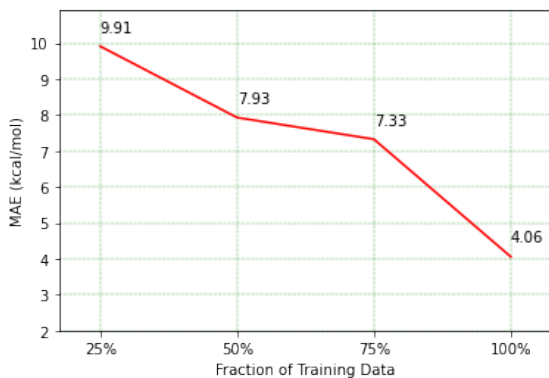


Figure 2: Mean absolute errors for atomization energy predictions at 0 K in kcal/mol on QM9 molecules with varying training set size.

Measure	A-FP	MPNN	MOLFORMER-XL Frozen	MOLFORMER-XL Finetuned
QM8 (avg MAE)	0.0282	0.0143	0.0155	0.0104
ESOL (RMSE)	0.503	0.58	0.472	0.3805
FreeSolv (RMSE)	0.736	1.15	0.538	0.4215

Table 4: MOLFORMER performance on QM8, ESOL, & FreeSolv benchmarks. Baseline performances are taken from references [Wu et al. \(2018\)](#); [Xiong et al. \(2019\)](#).

80%/10%/10% train/validation/test split as suggested in [Wu et al. \(2018\)](#). MOLFORMER-XL upon task-specific fine-tuning outperforms the baselines on all three benchmarks by a significant margin, confirming the generalization ability of MOLFORMER representation.

5 Conclusion

In this work, we have explored the potential of large-scale pre-trained molecular language models for property prediction tasks, for which knowing the precise molecular structure is important. Unlike graphs, molecular languages such as SMILES do not explicitly encode the complete structural information. However, with a well-designed self-supervised training on a large-scale corpus and an expressive architecture, such as a contextualized language model with an efficient linear attention mechanism, and a highly parallelized and specialized training protocol, our MOLFORMER can learn rich implicit structure-property relationship information from the large and diverse corpus of unlabeled molecules. Specifically, MOLFORMER significantly outperforms existing baselines that learn from inter-atomic distances or from message passing neural nets with limited expressivity, while keeping up with the more powerful but less scalable GNNs, for the highly accurate quantum chemical benchmarks. To our knowledge, this is the first work that validates the power of large scale self-supervised pre-trained molecular language models on electronic property prediction tasks.

On the large scale learning end, we showcased with MOLFORMER an efficient and an environment friendly use of computational resources, reducing the number of GPUs needed to perform the training by a factor of 60 (1000 vs 16).

MOLFORMER line of work has immediate potential for faster in silico screening of molecules across diverse targets, which is important for material design and drug discovery applications with crucial positive societal impact. The present work calls for further exploration of the representational power of MOLFORMER in the context of its ability to learn graph structural information from molecular language, which can be extended beyond the small organic molecules studied in this work. Future work will also aim at improving MOLFORMER by employing larger models as well as larger training data, using more well-designed and/or domain-specific self-supervised tasks, and by using other string based representations like SELFIES [Krenn et al. \(2020\)](#).

When using MOLFORMER for computational screening of molecules, it is possible for the model to be used in identifying potentially harmful chemicals. However, it should be noted that any realization of the MOLFORMER predictions need wet lab validation.

References

- APEX, online (2021). APEX: a pytorch extension with nvidia-maintained utilities to streamline mixed precision and distributed training. <https://github.com/NVIDIA/apex>. [Online; accessed 28-May-2021].
- Beltagy, I., Peters, M. E., and Cohan, A. (2020). Longformer: The long-document transformer. *arXiv:2004.05150*.
- Bjerrum, E. J. (2017). Smiles enumeration as data augmentation for neural network modeling of molecules.
- Chen, P., Liu, W., Hsieh, C.-Y., Chen, G., and Zhang, S. (2019). Utilizing edge features in graph neural networks via variational information maximization. *1906.05488*.
- Chithrananda, S., Grand, G., and Ramsundar, B. (2020). Chemberta: Large-scale self-supervised pretraining for molecular property prediction.
- Choromanski, K., Likhoshesterov, V., Dohan, D., Song, X., Gane, A., Sarlós, T., Hawkins, P., Davis, J., Mohiuddin, A., Kaiser, L., Belanger, D., Colwell, L., and Weller, A. (2020). Rethinking attention with performers. *CoRR*, abs/2009.14794.
- Coley, C. W., Barzilay, R., Green, W. H., Jaakkola, T. S., and Jensen, K. F. (2017). Convolutional embedding of attributed molecular graphs for physical property prediction. *Journal of chemical information and modeling*, 57(8):1757–1772.
- Defferrard, M., Bresson, X., and Vandergheynst, P. (2017). Convolutional neural networks on graphs with fast localized spectral filtering.
- Delaney, J. S. (2004). Esol: estimating aqueous solubility directly from molecular structure. *Journal of chemical information and computer sciences*, 44(3):1000–1005.
- Devlin, J., Chang, M., Lee, K., and Toutanova, K. (2018). BERT: pre-training of deep bidirectional transformers for language understanding. *CoRR*, abs/1810.04805.
- Devlin, J., Chang, M.-W., Lee, K., and Toutanova, K. (2019). BERT: Pre-training of deep bidirectional transformers for language understanding. In *Proceedings of the 2019 Conference of the North American Chapter of the Association for Computational Linguistics: Human Language Technologies, Volume 1 (Long and Short Papers)*, pages 4171–4186, Minneapolis, Minnesota. Association for Computational Linguistics.
- Duvenaud, D., Maclaurin, D., Aguilera-Iparraguirre, J., Gómez-Bombarelli, R., Hirzel, T., Aspuru-Guzik, A., and Adams, R. P. (2015a). Convolutional networks on graphs for learning molecular fingerprints. *arXiv preprint arXiv:1509.09292*.
- Duvenaud, D., Maclaurin, D., Aguilera-Iparraguirre, J., Gómez-Bombarelli, R., Hirzel, T., Aspuru-Guzik, A., and Adams, R. P. (2015b). Convolutional networks on graphs for learning molecular fingerprints. In *Proceedings of the 28th International Conference on Neural Information Processing Systems - Volume 2, NIPS'15*, page 2224–2232.
- Elnaggar, A., Heinzinger, M., Dallago, C., Rehawi, G., Wang, Y., Jones, L., Gibbs, T., Feher, T., Angerer, C., Steinegger, M., Bhowmik, D., and Rost, B. (2021). Prottrans: Towards cracking the language of life's code through self-supervised learning. *bioRxiv*.
- Falcon, WA, e. a. (2019). Pytorch lightning. *GitHub*. Note: <https://github.com/PyTorchLightning/pytorch-lightning>, 3.
- Gilmer, J., Schoenholz, S. S., Riley, P. F., Vinyals, O., and Dahl, G. E. (2017). Neural message passing for quantum chemistry.

- Goh, G. B., Hodas, N. O., Siegel, C., and Vishnu, A. (2017). Smiles2vec: An interpretable general-purpose deep neural network for predicting chemical properties. *arXiv preprint arXiv:1712.02034*.
- Gori, M., Monfardini, G., and Scarselli, F. (2005). A new model for learning in graph domains. In *Proceedings. 2005 IEEE International Joint Conference on Neural Networks, 2005.*, volume 2, pages 729–734 vol. 2.
- Hamilton, W. L., Ying, R., and Leskovec, J. (2018). Inductive representation learning on large graphs.
- Irwin, J. J. and Shoichet, B. K. (2005). ZINC—a free database of commercially available compounds for virtual screening. *Journal of Chemical Information and Modeling*, 45(1):177–182.
- Jo, J., Kwak, B., Choi, H.-S., and Yoon, S. (2020). The message passing neural networks for chemical property prediction on smiles. *Methods*, 179:65–72. Interpretable machine learning in bioinformatics.
- Katharopoulos, A., Vyas, A., Pappas, N., and Fleuret, F. (2020). Transformers are rnns: Fast autoregressive transformers with linearattention. *CoRR*, abs/2006.16236.
- Ke, G., He, D., and Liu, T.-Y. (2021). Rethinking positional encoding in language pre-training. In *International Conference on Learning Representations*.
- Kim, S., Chen, J., Cheng, T., Gindulyte, A., He, J., He, S., Li, Q., Shoemaker, B. A., Thiessen, P. A., Yu, B., Zaslavsky, L., Zhang, J., and Bolton, E. E. (2018). PubChem 2019 update: improved access to chemical data. *Nucleic Acids Research*, 47(D1):D1102–D1109.
- Kipf, T. N. and Welling, M. (2017). Semi-supervised classification with graph convolutional networks.
- Kitaev, N., Kaiser, L., and Levskaya, A. (2020). Reformer: The efficient transformer. In *International Conference on Learning Representations*.
- Klicpera, J., Groß, J., and Günnemann, S. (2020). Directional message passing for molecular graphs.
- Krenn, M., Häse, F., Nigam, A., Friederich, P., and Aspuru-Guzik, A. (2020). Self-referencing embedded strings (SELFIES): A 100% robust molecular string representation. *Machine Learning: Science and Technology*, 1(4):045024.
- Li, Y., Tarlow, D., Brockschmidt, M., and Zemel, R. (2015). Gated graph sequence neural networks. *arXiv preprint arXiv:1511.05493*.
- Liao, R., Zhao, Z., Urtasun, R., and Zemel, R. S. (2019). Lanczosnet: Multi-scale deep graph convolutional networks.
- Liu, S., Demirel, M. F., and Liang, Y. (2019a). N-gram graph: Simple unsupervised representation for graphs, with applications to molecules.
- Liu, Y., Ott, M., Goyal, N., Du, J., Joshi, M., Chen, D., Levy, O., Lewis, M., Zettlemoyer, L., and Stoyanov, V. (2019b). Roberta: A robustly optimized bert pretraining approach. *arXiv preprint arXiv:1907.11692*.
- Liu, Y., Wang, L., Liu, M., Zhang, X., Oztekin, B., and Ji, S. (2021). Spherical message passing for 3d graph networks.
- Maron, H., Ben-Hamu, H., Serviansky, H., and Lipman, Y. (2020). Provably powerful graph networks.
- Mobley, D. L. and Guthrie, J. P. (2014). Freesolv: a database of experimental and calculated hydration free energies, with input files. *Journal of computer-aided molecular design*, 28(7):711–720.
- Morris, C., Ritzert, M., Fey, M., Hamilton, W. L., Lenssen, J. E., Rattan, G., and Grohe, M. (2019). Weisfeiler and leman go neural: Higher-order graph neural networks. In *Proceedings of the AAAI Conference on Artificial Intelligence*, volume 33, pages 4602–4609.
- Öztürk, H., Özgür, A., and Ozkirimli, E. (2018). Deepdta: deep drug–target binding affinity prediction. *Bioinformatics*, 34(17):i821–i829.

- Paszke, A., Gross, S., Massa, F., Lerer, A., Bradbury, J., Chanan, G., Killeen, T., Lin, Z., Gimelshein, N., Antiga, L., Desmaison, A., Köpf, A., Yang, E., DeVito, Z., Raison, M., Tejani, A., Chilamkurthy, S., Steiner, B., Fang, L., Bai, J., and Chintala, S. (2019). Pytorch: An imperative style, high-performance deep learning library.
- Paul, A., Jha, D., Al-Bahrani, R., Liao, W.-k., Choudhary, A., and Agrawal, A. (2018). Chemixnet: Mixed dnn architectures for predicting chemical properties using multiple molecular representations. *arXiv preprint arXiv:1811.08283*.
- Raffel, C., Shazeer, N., Roberts, A., Lee, K., Narang, S., Matena, M., Zhou, Y., Li, W., and Liu, P. J. (2020a). Exploring the limits of transfer learning with a unified text-to-text transformer. *Journal of Machine Learning Research*, 21(140):1–67.
- Raffel, C., Shazeer, N., Roberts, A., Lee, K., Narang, S., Matena, M., Zhou, Y., Li, W., and Liu, P. J. (2020b). Exploring the limits of transfer learning with a unified text-to-text transformer. *Journal of Machine Learning Research*, 21(140):1–67.
- Ramakrishnan, R., Hartmann, M., Tapavicza, E., and von Lilienfeld, O. A. (2015). Electronic spectra from tddft and machine learning in chemical space. *The Journal of Chemical Physics*, 143(8):084111.
- RDKit, online (2021). RDKit: Open-source cheminformatics. <http://www.rdkit.org>. [Online; accessed 28-May-2021].
- Rives, A., Meier, J., Sercu, T., Goyal, S., Lin, Z., Liu, J., Guo, D., Ott, M., Zitnick, C. L., Ma, J., and Fergus, R. (2020). Biological structure and function emerge from scaling unsupervised learning to 250 million protein sequences. *bioRxiv*.
- Rogers, D. and Hahn, M. (2010). Extended-connectivity fingerprints. *Journal of chemical information and modeling*, 50(5):742–754.
- Rong, Y., Bian, Y., Xu, T., Xie, W., Wei, Y., Huang, W., and Huang, J. (2020). Self-supervised graph transformer on large-scale molecular data.
- Ruddigkeit, L., Van Deursen, R., Blum, L. C., and Reymond, J.-L. (2012). Enumeration of 166 billion organic small molecules in the chemical universe database gdb-17. *Journal of chemical information and modeling*, 52(11):2864–2875.
- Rupp, M., Tkatchenko, A., Müller, K.-R., and Von Lilienfeld, O. A. (2012a). Fast and accurate modeling of molecular atomization energies with machine learning. *Physical review letters*, 108(5):058301.
- Rupp, M., Tkatchenko, A., Müller, K.-R., and von Lilienfeld, O. A. (2012b). Fast and accurate modeling of molecular atomization energies with machine learning. *Phys. Rev. Lett.*, 108:058301.
- Schlichtkrull, M., Kipf, T. N., Bloem, P., van den Berg, R., Titov, I., and Welling, M. (2017). Modeling relational data with graph convolutional networks.
- Schütt, K. T., Arbabzadah, F., Chmiela, S., Müller, K. R., and Tkatchenko, A. (2017). Quantum-chemical insights from deep tensor neural networks. *Nature communications*, 8(1):1–8.
- Schütt, K. T., Kindermans, P.-J., Sauceda, H. E., Chmiela, S., Tkatchenko, A., and Müller, K.-R. (2017). Schnet: A continuous-filter convolutional neural network for modeling quantum interactions. In *Proceedings of the 31st International Conference on Neural Information Processing Systems, NIPS'17*, page 992–1002, Red Hook, NY, USA. Curran Associates Inc.
- Schwaller, P., Laino, T., Gaudin, T., Bolgar, P., Hunter, C. A., Bekas, C., and Lee, A. A. (2019). Molecular transformer: A model for uncertainty-calibrated chemical reaction prediction. *ACS Central Science*, 5(9):1572–1583.
- Shaw, P., Uszkoreit, J., and Vaswani, A. (2018). Self-attention with relative position representations. In *Proceedings of the 2018 Conference of the North American Chapter of the Association for Computational Linguistics: Human Language Technologies, Volume 2 (Short Papers)*, pages 464–468, New Orleans, Louisiana. Association for Computational Linguistics.

- Shin, B., Park, S., Kang, K., and Ho, J. C. (2019). Self-attention based molecule representation for predicting drug-target interaction. In *Machine Learning for Healthcare Conference*, pages 230–248. PMLR.
- Su, J., Lu, Y., Pan, S., Wen, B., and Liu, Y. (2021). Roformer: Enhanced transformer with rotary position embedding.
- Team, P. L. (2020). PyTorch Lightning 1.1 - Model Parallelism Training and More Logging Options. <https://bit.ly/3vA32ys>.
- Unke, O. T. and Meuwly, M. (2019). Physnet: A neural network for predicting energies, forces, dipole moments, and partial charges. *Journal of Chemical Theory and Computation*, 15(6):3678–3693.
- Vaswani, A., Shazeer, N., Parmar, N., Uszkoreit, J., Jones, L., Gomez, A. N., Kaiser, L., and Polosukhin, I. (2017). Attention is all you need. *arXiv:1706.03762*.
- Veličković, P., Cucurull, G., Casanova, A., Romero, A., Liò, P., and Bengio, Y. (2018). Graph attention networks. *arxiv, 1710.10903*.
- Vig, J., Madani, A., Varshney, L. R., Xiong, C., Socher, R., and Rajani, N. F. (2020). Bertology meets biology: Interpreting attention in protein language models. *arXiv preprint arXiv:2006.15222*.
- Vignac, C., Loukas, A., and Frossard, P. (2020). Building powerful and equivariant graph neural networks with structural message-passing.
- Wang, S., Guo, Y., Wang, Y., Sun, H., and Huang, J. (2019). Smiles-bert: Large scale unsupervised pre-training for molecular property prediction. In *Proceedings of the 10th ACM International Conference on Bioinformatics, Computational Biology and Health Informatics*, page 429–436. Association for Computing Machinery.
- Wang, S., Li, B. Z., Khabisa, M., Fang, H., and Ma, H. (2020). Linformer: Self-attention with linear complexity.
- Weininger, D. (1988). Smiles, a chemical language and information system. 1. introduction to methodology and encoding rules. *Journal of chemical information and computer sciences*, 28(1):31–36.
- Wolf, T., Lhoest, Q., von Platen, P., Jernite, Y., Drame, M., Plu, J., Chaumond, J., Delangue, C., Ma, C., Thakur, A., Patil, S., Davison, J., Scao, T. L., Sanh, V., Xu, C., Patry, N., McMillan-Major, A., Brandeis, S., Gugger, S., Lagunas, F., Debut, L., Funtowicz, M., Moi, A., Rush, S., Schmidt, P., Cistac, P., Muštar, V., Boudier, J., and Tordjmann, A. (2020). Datasets. *GitHub. Note: https://github.com/huggingface/datasets*, 1.
- Wu, Z., Ramsundar, B., Feinberg, E. N., Gomes, J., Geniesse, C., Pappu, A. S., Leswing, K., and Pande, V. (2018). Moleculenet: A benchmark for molecular machine learning.
- Xiong, Z., Wang, D., Liu, X., Zhong, F., Wan, X., Li, X., Li, Z., Luo, X., Chen, K., Jiang, H., et al. (2019). Pushing the boundaries of molecular representation for drug discovery with the graph attention mechanism. *Journal of medicinal chemistry*, 63(16):8749–8760.
- Xue, D., Zhang, H., Xiao, D., Gong, Y., Chuai, G., Sun, Y., Tian, H., Wu, H., Li, Y., and Liu, Q. (2020). X-mol: large-scale pre-training for molecular understanding and diverse molecular analysis. *bioRxiv*.
- You, Y., Li, J., Reddi, S., Hseu, J., Kumar, S., Bhojanapalli, S., Song, X., Demmel, J., Keutzer, K., and Hsieh, C.-J. (2019). Large batch optimization for deep learning: Training bert in 76 minutes. *arXiv preprint arXiv:1904.00962*.

A Appendix

We give here additional details and experiments to support our findings in the paper.

B Mean and Standard Deviation for Prediction Results Across Different Data Folds

The two major high-level variants of MOLFORMER are based on whether the weights of the base MOLFORMER is frozen or trained during the finetuning process of downstream tasks. Throughout the paper, these setups are referred to as either ‘Frozen’ or ‘Finetuned’, respectively.

We report the mean and standard deviations of MAE for 5 different folds of the data split into 80 % training and 10 % validation and 10% test. Most of the related work does not perform cross validation and just report the results on a single split. We note that the standard deviations are quite low for most of the predictions, suggesting the robustness of MOLFORMER representations. We also note that the mean error is higher for some of the tasks, than reported in the main paper. We believe this is because of the randomness in the splits and because we could not do extensive hyperparameter tuning on all the five splits for each measure.

PubChem Only				
Measure ↓	Frozen × Rotary	Frozen ✓ Rotary	Finetuned × Rotary	Finetuned ✓ Rotary
α	1.5915 ± 0.0413	1.4379 ± 0.0168	0.6661 ± 0.0685	0.6575 ± 0.0509
C_v	0.9852 ± 0.0261	0.8995 ± 0.0269	0.1641 ± 0.0665	0.1607 ± 0.0058
G	1.7218 ± 0.1061	2.3068 ± 0.1276	1.2877 ± 0.3059	1.4234 ± 0.2985
gap	0.0182 ± 0.0003	0.0174 ± 0.0002	0.0052 ± 0.0002	0.0051 ± 0.0001
H	2.2200 ± 0.0652	2.1615 ± 0.2438	1.3401 ± 0.2877	1.4220 ± 0.3053
ϵ_{homo}	0.0115 ± 0.0001	0.0111 ± 0.0001	0.0036 ± 0.0005	0.0036 ± 0.0001
ϵ_{lumo}	0.0148 ± 0.0002	0.0141 ± 0.0001	0.0034 ± 0.0001	0.0033 ± 0.0001
μ	0.8670 ± 0.0212	0.8505 ± 0.0157	0.4210 ± 0.0043	0.4257 ± 0.0083
$\langle R^2 \rangle$	87.6172 ± 1.7076	77.5032 ± 1.4228	24.3940 ± 2.1510	24.9213 ± 2.5526
U_0	1.9149 ± 0.1942	1.9247 ± 0.0941	1.3295 ± 0.2696	1.4516 ± 0.2722
U	1.8106 ± 0.1409	1.7770 ± 0.1462	1.3926 ± 0.1379	1.3366 ± 0.3006
ZPVE	0.0021 ± 0.0002	0.0017 ± 0.0001	0.0008 ± 0.0001	0.0008 ± 0.0001

Table 5: Mean and standard deviation of Mean Absolute Error (MAE) on the various QM9 tasks using a pretrained model that is trained on PubChem only.

PubChem+Zinc				
Measure ↓	Frozen × Rotary	Frozen ✓ Rotary	Finetuned × Rotary	Finetuned ✓ Rotary
α	0.6468 ± 0.0169	1.2956 ± 0.0244	0.7175 ± 0.0394	0.5784 ± 0.0419
C_v	0.2825 ± 0.0078	0.7959 ± 0.0141	0.2080 ± 0.0340	0.2447 ± 0.0363
G	1.2865 ± 0.1192	2.1535 ± 0.0503	1.9410 ± 0.4821	1.4406 ± 0.2396
gap	0.0089 ± 0.0000	0.0165 ± 0.0002	0.0053 ± 0.0001	0.0040 ± 0.0001
H	1.0730 ± 0.3188	1.8490 ± 0.1469	1.9430 ± 0.5519	1.3273 ± 0.2465
ϵ_{homo}	0.0066 ± 0.0000	0.0103 ± 0.0001	0.0042 ± 0.0003	0.0030 ± 0.0001
ϵ_{lumo}	0.0063 ± 0.0000	0.0128 ± 0.0001	0.0039 ± 0.0002	0.0029 ± 0.0001
μ	0.6872 ± 0.0049	0.8089 ± 0.0205	0.4368 ± 0.0133	0.4166 ± 0.0113
$\langle R^2 \rangle$	29.3779 ± 0.2944	72.8752 ± 1.1180	27.4802 ± 0.7409	27.0184 ± 1.6938
U_0	1.2877 ± 0.2373	2.1030 ± 0.0967	1.9210 ± 0.5015	1.2851 ± 0.1614
U	1.3238 ± 0.1954	1.8647 ± 0.0601	1.5565 ± 0.1809	1.3117 ± 0.1557
ZPVE	0.0005 ± 0.0000	0.0018 ± 0.0001	0.0005 ± 0.0001	0.0005 ± 0.0001

Table 6: Mean and standard deviation of Mean Absolute Error (MAE) on the various QM9 tasks using a pretrained model that is trained on both Pubchem and Zinc

C Assets and License

The following table summarizes the libraries utilized for our experiments and their accompanying license terms.

Asset	License	Link
Fast-Transformers	MIT License	https://github.com/idiap/fast-transformers/blob/master/LICENSE
Pytorch	BSD Style License	https://github.com/pytorch/pytorch/blob/master/LICENSE
RDKit	BSD 3-Clause "New" or "Revised" License	https://github.com/rdkit/rdkit/blob/master/license.txt
Pytorch Lightning	Apache 2.0 License	https://github.com/PyTorchLightning/pytorch-lightning/blob/master/LICENSE
HuggingFace Datasets	Apache 2.0 License	https://github.com/huggingface/datasets/blob/master/LICENSE
Nvidia APEX	BSD 3-Clause "New" or "Revised" License	https://github.com/NVIDIA/apex/blob/master/LICENSE

D Hyperparameters for Property Prediction

During the finetuning process, where the MOLFORMER as a feature extractor is not frozen, we experimented with different hyper-parameters. In our experiments, we found that batch sizes of both 64 and 128 work best for the downstreams tasks. Also, among various learning rates, 3e-5 seems to be the best fit for all the measures on QM9 dataset. The discriminator used was of a fixed size of 2 layers with a hidden size of 768 for all fine tuning experiments.

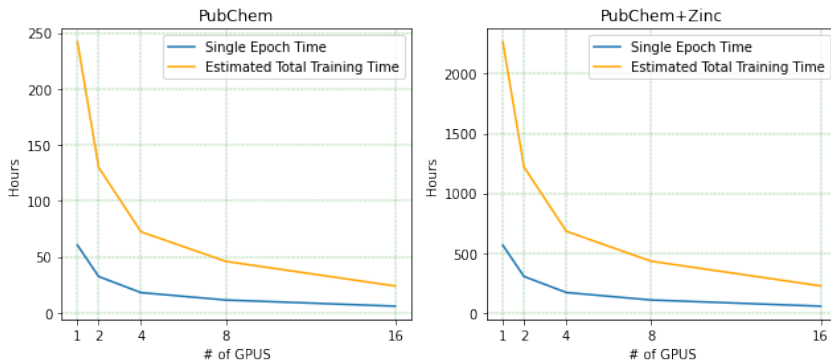
For the frozen strategy where the embeddings from the MOLFORMER is fixed, we use a fully connected model to predict the properties. A hyperparameter sweep was performed using grid search and we randomly picked 25 different variations for each task. The best model with the lowest validation loss was picked for further analysis. The different values of the hyperparameters are summarized in the table below.

Table 7: Different Values of the hyperparameters for the Frozen Models

Hyperparameter	Values
Learning Rate	0.001, 0.0001, 0.0005, 0.00005
Batch Size	64, 128, 256
Hidden Dimension	64, 128, 256, 512, 1024
Number of Layers	2, 3, 4

E PreTraining Scaleout

We give in Figure 1 the estimated training times of MOLFORMER as function of the used GPUs in the parrallelization.



(a) Estimated Pretraining Time

Figure 3: Estimated training times for our Linear attention MOLFORMER with *rotary* embeddings on a) PubChem and b) PubChem+ZINC datasets taken after 250 iterations. We see that training time decrease slightly sub-linearly as GPUs are added. Training time also scales approximately linearly as more data is added.

F Dataset, Vocabulary and Units

We have observed that various related work in the past uses different units for quantitative analysis on QM9 dataset without explicitly stating the units, and hence, often making it painful for the comparison. Owing to that reason, we have enlisted the units of the measures in the Table 8. We also give in Tables 9 and 10 the statistics of sequence length and vocabulary for the datasets considered in this work.

Measure	Unit
α	Bohr ³
C_v	cal/(mol*K)
G	Hartree
gap	Hartree
H	Hartree
ϵ_{homo}	Hartree
ϵ_{lumo}	Hartree
μ	Debye
$\langle R^2 \rangle$	Bohr ²
U_0	Hartree
U	Hartree
ZPVE	Hartree

Table 8: Units of QM9 target measures

Table 9: Minimum, maximum and mean and standard deviation of sequence length for the datasets considered in this work. The vocabulary size after tokenization is also given in the last column.

Pretrained Data	Min	Max	Mean	Std	Vocab Size
QM9	1	22	14.76	2.02	30
Pubchem	1	2211	49.13	24.90	2252
Zinc	4	152	43.08	8.70	113
Pubchem + Zinc	1	2211	44.76	14.55	2279

Table 10: Top five most frequent tokens for each data source.

Pretrained Data	Most Frequent Tokens
QM9	C, 1, 0, 2, (
Pubchem	C, =, (,), 0
Zinc	C, c, (,), 1
Pubchem + Zinc	C, c, (,), =